1st Pan-American Congress on Computational Mechanics – PANACM 2015
XI Argentine Congress on Computational Mechanics – MECOM 2015
S. Idelsohn, V. Sonzogni, A. Coutinho, M. Cruchaga, A. Lew & M. Cerrolaza (Eds)

BLADE CUTTING SIMULATION WITH CRACK PROPAGATION THROUGH THIN-WALLED STRUCTURES VIA SOLID-SHELL FINITE ELEMENTS IN EXPLICIT DYNAMICS

ALDO GHISI, FEDERICA CONFALONIERI AND UMBERTO PEREGO

Dipartimento di Ingegneria Civile e Ambientale, Politecnico di Milano
Piazza Leonardo da Vinci 32, 20133, Milano (ITALY)
aldo.ghisi@polimi.it, federica.confalonieri@polimi.it, umberto.perego@polimi.it

Key words: Solid Shell Finite Elements, Selective Mass Scaling, Layered Thin-Walled Structures, Explicit Dynamics, Blade Cutting.

Summary. *To simulate the crack propagation due to blade cutting of a thin-walled shell structure, we propose a numerical technique based on solid shell finite elements and explicit time integration. The limitation on the critical time step due to the small thickness along the out-of-plane direction is overcome through a selective mass scaling, capable to optimally define the artificial mass coefficient for distorted elements in finite strains: since the selective scaling cuts the undesired, spurious contributions from the highest eigenfreqeuencies, but saves the lowest frequencies associated to the structural response, and since the method preserves the lumped form of the mass matrix, the calculations in the time domain are conveniently speeded up. The interaction of the cutting blade with the cohesive process zone in the crack tip region is accounted for by means of the so-called directional cohesive interface concept. Unlike in previous implementations, through-the-thickness crack propagation is also considered. This is of critical importance in particular in the case of layered shells, where one solid-shell element per layer is used for the discretization in the thickness direction and it is a necessary ingredient for future possible consideration of delamination processes. We show by applying the proposed procedure to the cutting of a thin-walled laminate used for packaging applications that this is a promising tool for the prediction of the structural response of thin-walled structures in the presence of crack propagation induced by blade cutting.*

1 INTRODUCTION

In this paper we consider the simulation of the opening process of a thin laminate membrane sealing a carton package by means of cutting blades. This problem is actually challenging from a computational point of view, since the simulation must account for fracture initiation and propagation through a thin-walled laminate. The nonlinear material behaviour of the single layer and the small laminate thickness make recently introduced [1-2] approaches, based on solid-shell elements particularly attractive. Moreover, the dynamic nature of the fracture process and the severe nonlinearity due in particular to the interaction

with the cutting blade suggest to use an explicit dynamics time integration scheme. These issues require a detailed analysis of numerous numerical problems, whose solution is briefly recalled in the following sections. The simulation approach considered here is based on the directional cohesive element concept, first proposed in [14] to simulate blade-induced crack propagation in classical elastic shell elements and later reformulated for application to solid-shell elements [3]. Directional cohesive elements are special interface elements, to be interposed between adjacent shell elements, capable to account for the interaction between the cutting blade and the cohesive process zone. Section 2 briefly recalls the adopted solid-shell finite element formulation, section 3 details the selective mass scaling approach; in section 4 we sketch the ideas, i.e. the directional cohesive elements, at the base of the interaction between the cutting blade and the fracture resistance of the laminate, and in section 5 we show the application of the modelling to an opening laminate in the packaging industry.

2 SOLID SHELL ELEMENT FORMULATION

Solid-shell finite elements, unlike standard, structural shell elements make use of only translational degrees of freedom. Because of the three-dimensional kinematic formulation, the constitutive laws used for continuum, three-dimensional finite elements can be adopted as well, including direct consideration of thickness deformation. Unlike standard finite elements, solid-shell elements can be conveniently used for the discretization of layered thin-walled structures, by simple stacking a number of solid-shell elements, typically one or more per layer, one on top of the other through the shell thickness. In the following we choose the Q1STS finite element proposed by Schwarze and Reese [1-2], an eight-node hexahedron including a reduced integration and hourglass control, recently adapted to explicit dynamics in [6]. Solid-shell elements are affected by numerical problems, such as Poisson, volumetric, curvature and shear locking and by hourglassing, the latter due to reduced integration which is an important ingredient for an efficient explicit time integration scheme. In Schwarze and Reese implementation volumetric and Poisson's locking are dealt with by the enhanced assumed strain (EAS) approach, while the assumed natural strain (ANS) concept is used for the transverse shear and curvature thickness locking. Hourglassing is controlled by adding suitably constructed artificial stiffness.

3 SELECTIVE MASS SCALING

In explicit structural dynamics the advantage of algorithm simplicity (there are no linear systems to be solved) is balanced by the small allowed stable time step; in the case of the widely diffused central difference scheme, the time step Δt is dependent on the maximum eigenfrequency $\omega_{\max}$ of the finite element mesh according to

$$\Delta t \leq \frac{2}{\omega_{\max}} \tag{1}$$

in the undamped case [8]. $\omega_{\max}$ is in turn conservatively bounded by the maximum eigenfrequency of the single finite element $\omega_{\max}^{e}$:

$$\omega_{\max} \leq \max_{e}\{\omega_{\max}^{e}\}. \tag{2}$$

Moreover, because of the large difference between the thickness and the in-plane dimensions

of a shell, the Courant-Friedrichs-Lewy condition, limiting the time step to a fraction of the element traversal time of an elastic wave, leads to very small time increments in explicit dynamics. To overcome this severe limitation, the selective mass scaling concept can be pursued: the idea is to artificially alter the solid-shell element mass matrix in order to scale down the highest eigenfrequencies with small or negligible changes to the lowest ones. There are several approaches to achieve this goal (see e.g. [13,15,16,17,18,19]), but most of these ideas make the scaled mass matrix non diagonal, an undesirable outcome for explicit time integration schemes. Here we follow the approach shown in the series of papers [4,6,9,10], where the relative motion between the lower and upper shell surfaces of a 8-node three-linear, solid-shell element is conveniently penalized so that the smallness of the thickness is not determining the time step anymore. The approach maintains the translational rigid body inertia, while the rigid body rotational inertia is modified; therefore, it should be used with care when a significant component of the motion is a pure rigid body rotation. Besides this drawback, we emphasize that the method works for regular and distorted finite elements in finite strains [4].

3.1 Principles of the proposed selective scaling approach

To summarize our selective mass scaling approach we use here the notation described in [4]: it starts by introducing the splitting of the element nodal coordinates according to the upper and lower surface (see figure 1):

$$\boldsymbol{X} = \begin{bmatrix} \boldsymbol{X}_{1-4} \\ \boldsymbol{X}_{5-8} \end{bmatrix}. \tag{3}$$

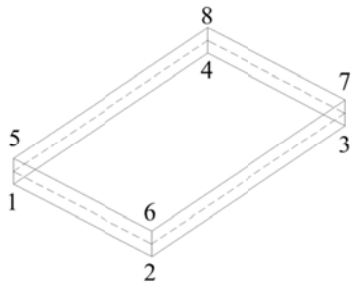

Figure 1: Local numbering adopted for the solid-shell element.

Then, the coordinates of the corner nodes at the middle surface and the corner fibers, i.e. the segments connecting the corresponding nodes of the upper and lower surface, are defined:

$$\boldsymbol{X}^m = \frac{\boldsymbol{X}_{5-8} + \boldsymbol{X}_{1-4}}{2} \qquad \Delta\boldsymbol{X} = \frac{\boldsymbol{X}_{5-8} - \boldsymbol{X}_{1-4}}{2} \tag{4a,4b}$$

and these items are collected in the transformed coordinate vector

$$\widehat{\boldsymbol{X}} = \begin{bmatrix} \boldsymbol{X}^m \\ \Delta\boldsymbol{X} \end{bmatrix} \tag{5}$$

which is related to the original coordinates via the linear transformation

$$\boldsymbol{X} = \boldsymbol{Q}\hat{\boldsymbol{X}} \qquad\qquad \boldsymbol{Q} = \begin{bmatrix} \mathfrak{I} & -\mathfrak{I} \\ \mathfrak{I} & \mathfrak{I} \end{bmatrix} \tag{6a,7b}$$

where $\mathfrak{I}$ is the 12x12 identity matrix. A similar transformation can be followed also for displacements, velocities and, finally, accelerations, which in particular read:

$$\boldsymbol{a} = \begin{bmatrix} \boldsymbol{a}_{1-4} \\ \boldsymbol{a}_{5-8} \end{bmatrix}, \quad \hat{\boldsymbol{a}} = \begin{bmatrix} \boldsymbol{a}^m \\ \Delta\boldsymbol{a} \end{bmatrix} \qquad\qquad \boldsymbol{a} = \boldsymbol{Q}\hat{\boldsymbol{a}}. \tag{8a-c}$$

The principle of virtual work for the motion of an undamped system can be therefore transformed as follows:

$$\delta\hat{\boldsymbol{a}}_e^T \, \widehat{\boldsymbol{M}}^{\alpha}_{e,\text{lumped}} \, \hat{\boldsymbol{a}}_e = \delta\hat{\boldsymbol{a}}_e^T \, \hat{\boldsymbol{f}}_e \tag{9}$$

with $\delta\hat{\boldsymbol{a}}_e$ equal to the transformed virtual acceleration of the nodes of element *e*, $\hat{\boldsymbol{f}}_e = \hat{\boldsymbol{f}}_e^{ext} - \hat{\boldsymbol{f}}_e^{int}$ the difference between external and internal (transformed) equivalent nodal forces for the single FE, and $\widehat{\boldsymbol{M}}^{\alpha}_{e,\text{lumped}}$ the lumped form of the selectively scaled mass matrix, namely

$$\widehat{\boldsymbol{M}}^{\alpha}_{e,\text{lumped}} = \begin{bmatrix} \boldsymbol{m}^{up} + \boldsymbol{m}^{low} & \boldsymbol{0} \\ \boldsymbol{0} & \alpha^e(\boldsymbol{m}^{up} + \boldsymbol{m}^{low}) \end{bmatrix} \tag{10}$$

$\boldsymbol{m}^{up}$ and $\boldsymbol{m}^{low}$ being 12x12 diagonal matrices collecting the element nodal masses at the upper and lower surface nodes, respectively, and α^e being the element scaling coefficient. Notice that α^e is applied only to the difference in nodal acceleration between the upper and lower surface and not to the middle surface nodal accelerations that are responsible for the element translational rigid body motion. In case of a single layer thin-walled structure, this mass matrix evidently does not change the diagonal form of the problem and can be directly inserted in the explicit solver routines written in the transformed variables. In case, instead, of a layered structure, it is necessary to reverse to original coordinates; in fact, after assembly, the nodal masses of adjacent layers belonging to the same multi-layer fiber sum up, thus requiring to solve a small linear system. While a detailed presentation is present in [9], the basic idea can be grasped by considering the three layers (labelled as *a*, *b*, *c*) example in figure 2. For each fiber *f* in this case the problem to be solved is

$$\boldsymbol{M}_f^{\alpha} \, \boldsymbol{a}_f = \boldsymbol{f}_f \tag{11}$$

with

$$\boldsymbol{M}_f^{\alpha} = \begin{bmatrix} \boldsymbol{m}_a^{LL} & \boldsymbol{m}_a^{LU} & \boldsymbol{0} & \boldsymbol{0} \\ \boldsymbol{m}_a^{UL} & \boldsymbol{m}_a^{UU} + \boldsymbol{m}_b^{LL} & \boldsymbol{m}_b^{LU} & \boldsymbol{0} \\ \boldsymbol{0} & \boldsymbol{m}_b^{UL} & \boldsymbol{m}_b^{UU} + \boldsymbol{m}_c^{LL} & \boldsymbol{m}_c^{LU} \\ \boldsymbol{0} & \boldsymbol{0} & \boldsymbol{m}_c^{UL} & \boldsymbol{m}_c^{UU} \end{bmatrix}$$

and $\boldsymbol{m}_l^{LL} = \boldsymbol{m}_l^{UU} = \sum(1+\alpha^e)\,(\boldsymbol{m}^{up} + \boldsymbol{m}^{low})$, $\boldsymbol{m}_l^{LU} = \boldsymbol{m}_l^{UL} = \sum(1-\alpha^e)\,(\boldsymbol{m}^{up} + \boldsymbol{m}^{low})$, where, for each node, the sum operator has to be interpreted as the assembly over the layer *l=a,b,c* of the elements sharing that node.

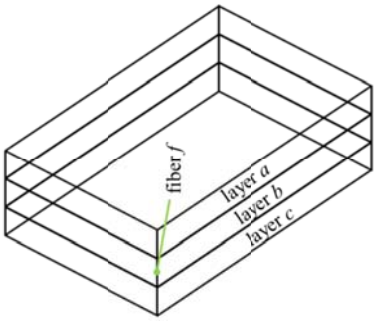

Figure 2: Three-layers laminate.

3.2 Optimal mass scaling factor

Unnecessary high values of the scaling coefficient α can overly modify the structural dynamical properties (e.g. rigid body rotational inertia) and it can be shown [9] that the dependence of the maximum eigenfrequency on the mass scaling coefficient actually shows a plateau for increasing α. Therefore, it is necessary to determine the optimal scaling: this problem has been solved in [10] for parallelepiped elements and in [4] for distorted elements, essentially by exploiting the equivalence between selective scaling and element thickness geometrical scaling. A good approximation of the optimal estimate for the mass scaling coefficient turns out to be:

$$\alpha^{\text{opt}} \cong \frac{L_{\text{min}}^2}{h_0^2} \tag{12}$$

where $L_{\text{min}} = \min\{L_1, L_2\}$ is the minimum in-plane length and h_0 is the thickness of the solid-shell element. The estimate is actually exact for parallelepiped elements while only approximate for distorted elements (in [4] the exact solution is provided for interested readers). Moreover, this estimate is different for each layer of the laminate and for each element; by using the more restricted estimate, the time step depends only on the element in-plane dimensions and not on its thickness. To pass from the mass scaling coefficient stated in equation 12 to the time step estimate, we follow equations 1 and 2 where ω_{max}^e is conveniently bounded (details are given in [4]) by the solution of the element eigenvalue problem $f(\omega^2; \alpha^{\text{opt}}) = 0$ via a Newton-Raphson procedure.

4 DIRECTIONAL COHESIVE ELEMENTS

A sharp blade cutting a ductile (or not purely brittle) material can interact with the cohesive process zone during crack propagation. In this case, a classical implementation of the cohesive approach would lead to incorrect results unless an extermely fine, computationally prohibitive mesh, capable to resolve the blade radius of curvature, were used. The "directional" cohesive approach [3,14] is intended to provide a macroscopic but energetically consistent description of this interaction, allowing a crack to propagate along element interfaces where special string elements are inserted after node duplication. Under the assumptions of i) neglecting the bending strength of individual layers because of their small thickness, and ii) the independence of the specific surface work due to cutting from the crack

propagation mode (this implies that only fracture mode I is relevant, once the fracture criterion is met at a given node), one massless cable per layer is introduced between the separating element faces in correspondence of the element middle surfaces. The cable element is a geometric entity, capable to detect contact and to interact with the advancing cutting blade (figure 3a, 3b): the latter, in fact, modifies the original straight configuration of the cable, by generating a joint in correspondence of the contact point at the cutting edge (the possibility of contact with the lateral surfaces of the blade is excluded because of the assumed sharpness of the cutting blade), and allowing for a transmission of the cohesive force in the correct direction.

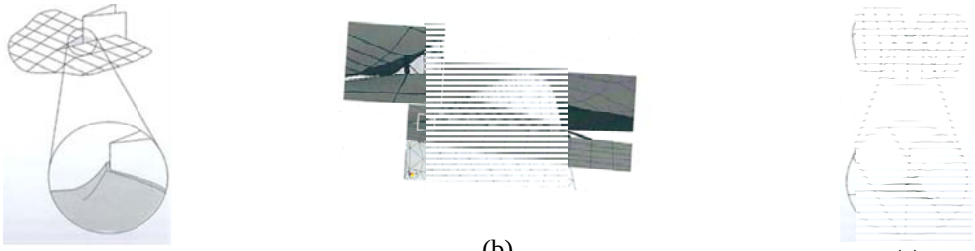

(a) (b) (c)

Figure 3: (a) blade cutting through the mesh, (b) interaction of the blade with the cable elements, and (c) "directional" cohesive forces.

Unlike in the classical cohesive approach, these forces have different directions on the two separating crack flanks, determined by the directions of the truss elements connecting the solid-shell nodes with the cable joint (see figures 3c and 4b). By assuming that the blade position is given at each time, then the contact point $\boldsymbol{x}^m$ between blade and cable and the displacement discontinuities $\boldsymbol{\delta}^m$ are known at the end of each explicit time integration step, so that the cohesive forces become:

$$\boldsymbol{f}_a^+ = \frac{\|\boldsymbol{f}_a\|}{\|\boldsymbol{x}^m - \boldsymbol{x}^{\mathrm{mid}+}\|}\left(\boldsymbol{x}^m - \boldsymbol{x}^{\mathrm{mid}+}\right)$$
$$\boldsymbol{f}_a^- = \frac{\|\boldsymbol{f}_a\|}{\|\boldsymbol{x}^m - \boldsymbol{x}^{\mathrm{mid}-}\|}\left(\boldsymbol{x}^m - \boldsymbol{x}^{\mathrm{mid}-}\right) \qquad (13a,13b)$$

where the subscripts "+" and "-" denote opposite crack flanks, $\boldsymbol{x}^m$ is the contact point between the cable and the blade and $\boldsymbol{x}^{\mathrm{mid}}$ is the point of the crack flank where the cable is attached in correspondence of the element middle surface.

The forces $\boldsymbol{f}_a$ are calculated from the cohesive model described in [20], assuming a linear softening law relating the opening traction T to a scalar measure of the crack opening ℓ and a cohesive potential $G(\ell, q)$ with q an internal variable, shown in figure 4a for the simple case of a linear softening law, i.e. the maximum attained crack opening, also interpreted as a progressive damage inside the process zone.

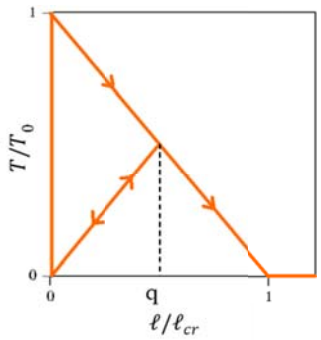

(a)

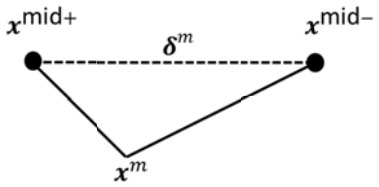

(b)

Figure 4: (a) softening cohesive law; (b) direction of cohesive forces during interaction with the blade.

A softening function $g(q)$ is also introduced so that, in the linear softening case, the cohesive law is written as follows:

$$\begin{gathered} G_f = \frac{1}{2} T_0 \, \ell_{cr} \\ G = G_f + \frac{1}{2}\frac{T_0}{q}\left(1 - \frac{q}{\ell_{cr}}\right)\ell^2 - T_0 q\left(1 - \frac{1}{2}\frac{q}{\ell_{cr}}\right) \\ g(q) = -\frac{\partial G}{\partial \ell}(0,q) = T_0\left(1 - \frac{q}{\ell_{cr}}\right) \\ T = \frac{\partial G}{\partial \ell}(\ell, q) = \frac{T_0}{q}\left(1 - \frac{q}{\ell_{cr}}\right)\ell = \frac{g(q)}{q}\ell \qquad \text{when } \ell \le q, \dot{q} = 0 \\ T = g(q) \qquad \text{when } \ell = q, \dot{q} \ge 0. \end{gathered} \tag{14a-e}$$

It is therefore obtained $\boldsymbol{f}_a = \boldsymbol{T}_a^{\text{mid}} A_a$, while $\ell = \left\|\boldsymbol{x}^m - \boldsymbol{x}^{\text{mid}+}\right\| + \left\|\boldsymbol{x}^m - \boldsymbol{x}^{\text{mid}-}\right\|$ is the length of the cable. The parameter T_0 is set equal to the component of the stress tensor in the direction normal to the opening faces of the element in the continuum model where the fracture criterion is met; ℓ_{cr}, is, instead, assumed to be a material parameter.

An equivalent plastic strain criterion, with a Heaviside function assuring that only tensile stresses contribute to the fracture, is adopted:

$$\varepsilon_{cr}^p = \int_0^{\varepsilon_f^p} H\left(\sigma_H\right) \mathrm{d}\varepsilon^p \tag{15}$$

where ε_f^p is the plastic strain value at fracture, σ_H is the hydrostatic stress accounting for the influence of triaxiality, and the crack direction coincides with the element edge closer to the maximum principal stress at the node where the criterion has been met.

5 RESULTS

The proposed approach has already proven itself promising in several single-layer applications [3,6]. Here we show an application to a multi-layered structure. The extension is not trivial because of the much higher complexity of the kinematics of the fracture opening during the through-the-thickness crack propagation.

A thin laminate membrane closes the carton package for fluid aliments [7] shown in figure 5. The circular hole to be produced through the applied cap equipped with high density polyethylene (HDPE) cutting teeth has the diameter of 15 mm: it is obtained with a torque applied by the user to the screw thread. In the remainder of the package the laminate constituting the hole does not contain paper, but only aluminum and low density polyethylene

(LDPE); this laminate has a thickness ranging from 70 to 78 μm, with the aluminum core 6-9 μm thick, while a LDPE layer coat this interior core from both sides.

(a) (b) (c)

Figure 5: (a) package with hole for opening, (b) package with the screw thread applied, (c) detail of the cutting teeth (upside down view).

In the modelling we assume a circular membrane with radius equal to 10.2 mm and thickness 0.074 mm. The 14% larger diameter accounts for the slackness of the actual membrane due to the manufacturing process. As shown in figure 5c, the cutting tool (referred to as the "blade" from now on) has a radius of 9.4 mm and its edges present a curvature radius of 0.1 mm (see also figure 6b). We consider the blade (figure 6a) as a rigid body whose motion is given: it has a rotation around its vertical axis and a translation along the same axis penetrating the three-layer membrane shown in figure 6b.

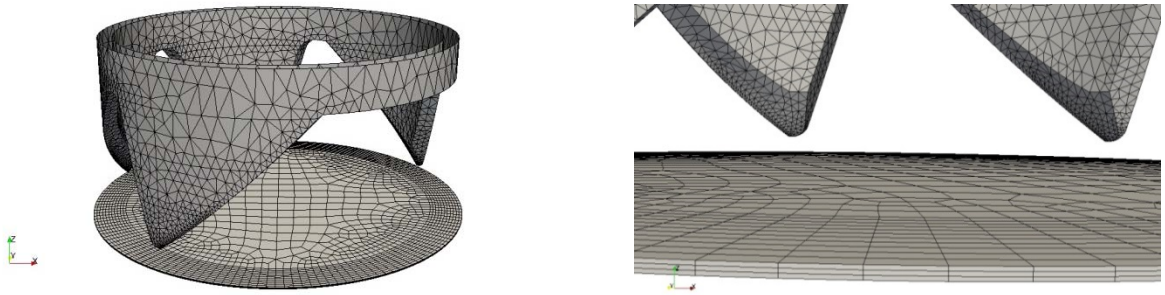

(a) (b)

Figure 6: (a) FE model of blade and membrane; (b) detail of the three layers membrane.

The composite laminate in this example is assumed as an equivalent and homogenized membrane with Young modulus E=176 GPa, Poisson's ratio ν=0.3 and density ρ=2·10^{-9} Ns^2/mm^4. A hardening behavior is adopted according to the yielding function

$$\sigma_y(\varepsilon^p) = \sigma_{y0} + Q\left(1 - \exp(-\varsigma\,\varepsilon^p)\right) \tag{27}$$

where σ_{y0}=11 MPa is the initial stress, the saturation parameter Q is equal to 40 MPa, and the hardening exponent ς=6.63. The chosen fracture parameters are G_f =30 N/mm and T_0= 18 MPa. The blades produces several cuts along their circular path as shown in figure 6a; the cut appearance (figure 7a) is in good qualitative agreement with experimental observations of the opening process, as much as the torque vs cap rotation response shown in figure 7b. This comparison shows that, neglecting the initial mismatch between the two curves, due to the

lack of friction imposed on the rotating teeth before contact with the laminate, the agreement is reasonable.

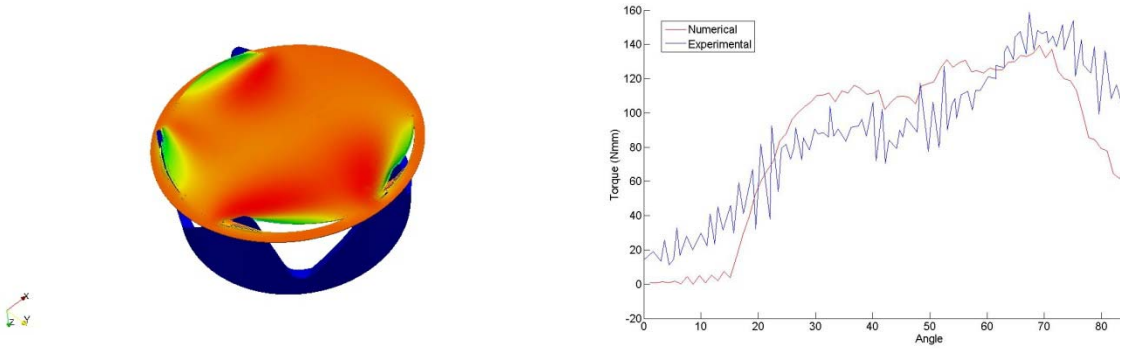

(a) (b)

Figure 7: (a) upside down view of the membrane cut by the blades;
(b) comparison between numerical and experimental torque during the rotation.

6 CONCLUSIONS

A simulation approach for the numerical evaluation of the opening process of a thin-walled laminate has been presented. It makes use of solid-shell elements enriched to correct known locking issues, in a finite strain formulation. To conveniently exploit the advantages of an explicit time integration scheme in structural dynamics, an effective selective mass scaling technique has been implemented, whereby only the highest eigenfrequencies responsible of the smallness of the time step are reduced. To correctly describe the interaction between the blade and the fracturing multi-layered thin-walled membrane, interface directional cohesive elements have been used. We have shown that several layers can be used for the description of the laminate, and fracture initiation and propagation in multi-layered structures is well represented; in the future the possible delamination between layers will be considered.

AKNOWLEDGMENTS

We are grateful for the support given by Tetra Pak Packaging Solutions.

REFERENCES

[1] Schwarze, M. and Reese, S. A reduced integration solid-shell finite element based on the EAS and the ANS concept – Large deformation problems. *International Journal for Numerical Methods in Engineering* (2011) **85**:289–329.

[2] Reese, S. A large deformation solid-shell concept based on reduced integration with hourglass stabilization. *International Journal for Numerical Methods in Engineering* (2007) **69**:1671-1716.

[3] Pagani, M. and Perego, U. Explicit dynamics simulation of blade cutting of thin elastoplastic shells using “directional” cohesive elements in solid-shell finite element models. *Computer Methods in Applied Mechanical and Engineering* (2015) **285**:515-541.

[4] Cocchetti, C., Pagani, M. and Perego, U. Selective mass scaling for distorted solid-shell elements in explicit dynamics: optimal scaling factor and stable time step estimate.

International Journal for Numerical Methods in Engineering (2015) DOI:10.1002/nme.

[5] Frangi, A., Pagani, M., Perego, U. and Borsari, R. Directional cohesive elements for the simulation of blade cutting of thin shells. *Comp. Model. Engng. & Sciences* (2010) **57**:205–224.

[6] Pagani, M., Reese, S. and Perego, U. Computationally efficient explicit nonlinear analyses using reduced integration-based solid-shell finite elements. *Computer Methods in Applied Mechanical and Engineering* (2014) **268**:141-159.

[7] Andreasson, E., Kao-Walter, S. and Sthåle, P. Micro-Mechanisms of a Laminated Packaging Material during fracture. *Engineering Fracture Mechanics* (2014) **127**:313-326.

[8] Belytschko, T. and Hughes, T.J.R. (eds), *Computational methods for Transient Analysis*, Elsevier Science Publishers B.V. (1983) 1–155.

[9] Confalonieri, F., Ghisi, A. and Perego, U. Solid-shell selective mass scaling for explicit dynamic analysis of layered thin-walled structures. *Submitted* (2015).

[10] Cocchetti, G, Pagani, M. and Perego, U. Selective mass scaling and critical time-step estimate for explicit dynamics analyses with solid-shell elements. *Computers & Structures* (2013) **127**:39–52.

[11] Simo, J.C. and Armero, F. Geometrically non-linear enhanced strain mixed methods and the method of incompatible modes, *International Journal for Numerical Methods in Engineering* (1992) **33**:1413–1449.

[12] Bischoff, M. and Ramm, E. Shear deformable shell elements for large strains and rotations, *International Journal for Numerical Methods in Engineering* (1997) **40**:4427–4449.

[13] Olovsson, L, Unosson, M. and Simonsson, K. Selective mass scaling for thin walled structures modeled with tri-linear solid elements, *Computational Mechanics* (2004) **34**:134–136.

[14] Frangi, A., Pagani, M., Perego, U. and Borsari, R. Directional Cohesive Elements for the Simulation of Blade Cutting of Thin Shells. *Computer Modeling in Engineering & Sciences* (2010) **57**:205-224.

[15] Olovsson, L., Simonsson K. and Unosson M. Selective mass scaling for explicit finite element analyses. *International Journal for Numerical Methods in Engineering* (2005) **63**:1436-1445.

[16] Macek, R.W. and Aubert. B.H. A mass penalty technique to control the critical time increment in explicit dynamic finite element analyses. *Earthquake Engineering and Structural Dynamics* (1995) **24**:1315-1331.

[17] Hetherington, J., Rodriguez-Ferran, A. and Askes, H. A new bipenalty formula- tion for ensuring time step stability in time domain computational dynamics. *International Journal for Numerical Methods in Engineering* (2012) **90**:269-286.

[18] Askes, H., Nguyen, D.C.D. and Tyas, A. Increasing the critical time step: micro-inertia, inertia penalties and mass scaling. *Computational Mechanics* (2011) **47**:657-667.

[19] Tkachuk, A. and Bischoff, M. Variational methods for selective mass scaling. *Computational Mechanics* (2013) **52**:563-570.

[20] Comi, C., Mariani, S., Negri, M. and Perego, U. A one-dimensional variational formulation for quasi-brittle fracture. *Journal of Mechanics of Material and Structures* (2006) **1**:1323-1343.